

INTERNATIONAL SOCIETY FOR SOIL MECHANICS AND GEOTECHNICAL ENGINEERING



This paper was downloaded from the Online Library of the International Society for Soil Mechanics and Geotechnical Engineering (ISSMGE). The library is available here:

<https://www.issmge.org/publications/online-library>

This is an open-access database that archives thousands of papers published under the Auspices of the ISSMGE and maintained by the Innovation and Development Committee of ISSMGE.

Shear and dissociation characteristics of methane hydrate bearing sand with fines

Caractéristiques de cisaillement et dissociation des gisements sableux d'hydrate de méthane contenant des fines

Shintaro Kajiyama

Department of Civil & Environmental Engineering, Yamaguchi University, Japan, u002wrf@yamaguchi-u.ac.jp

Masayuki Hyodo, Norimasa Yoshimoto

Graduate School of Sciences and Technology for Innovation, Yamaguchi University, Japan

ABSTRACT: The shearing and dissociation characteristics of methane hydrate (MH) bearing sands with different fines content were investigated using a high-pressure low-temperature plane strain testing apparatus. The initial stiffness and peak strength of MH bearing sands increased with increasing MH saturation. The strength increment due to the existence of MH increased with increasing fines content. After the hydrate dissociation induced by the depressurization method, the failure of MH bearing sands regardless of the fines content subjected to the initial shear stress continued with the axial strain progressed. The stress ratio of specimens after hydrate dissociation and the pore pressure recovery process was equal to that of host sand.

RÉSUMÉ : Les caractéristiques de cisaillement et dissociation des gisements sableux d'hydrate de méthane (MH) contenant des fines en proportions différentes ont été étudiées en déformations planes sous haute pression et basse température. On a trouvé que la rigidité initiale et le pic de cisaillement de ces gisements augmentent avec le niveau de saturation en MH. Le gain en résistance dû à l'existence de MH s'accroît avec la proportion de fines. Après la dissociation de l'hydrate provoquée par la méthode de dépressurisation, la rupture des sables porteurs de MH a continué sous la pression de cisaillement initiale avec une progression des déformations axiales, quel que soit la proportion de fines. Le rapport des contraintes après dissociation de l'hydrate et le procédé de rétablissement des pressions interstitielles étaient égaux à ceux du sable.

KEYWORDS: methane hydrate, fines

1 INTRODUCTION

Methane hydrate (hereafter referred to as MH) has been expected to become a future energy source in recent years. MH is confirmed in the deep sea bed at depths of over 1000 meters near Japan. Especially, it is assumed that the quantity of methane gas in Nankai Trough is equivalent to that of large gas field. In 2013, an offshore production test was carried out in order to investigate the feasibility of methane gas extraction from the sea bed for commercial purposes (MH21 Research Consortium, 2014). The geology of the sea bed of the Nankai Trough, called turbidite, constitutes multiple stratified layers of sand and clay (Suzuki, et al., 2009). MH mostly exists in the void spaces of the sand layers. The grain size distribution of MH bearing sand varies with location in the sea bed. In order to produce methane gas from the MH concentrated layers, it is particularly important to understand the mechanical and dissociation properties of MH bearing sand. A series of triaxial shearing and depressurization tests were performed on artificial MH bearing sands using a high-pressure and low-temperature plane strain testing apparatus developed by Hyodo et al. (Hyodo et al., 2013) to examine their shearing and dissociation characteristics. This high-pressure and plane strain testing apparatus equipped with an observation window was employed to understand not only the shear behaviour but also local deformation of specimens using Toyoura sand by Yoneda et al. (Yoneda et al., 2013). Three kinds of sands with different fines contents were used as the host sands for preparing the MH bearing sands in this study.

2 TEST APPARATUS AND TESTING PROCEDURE

In this study, Toyoura sand and two other kinds of silica sands named T_b and T_c , which were artificially prepared in accordance to the grain size distributions of sediments in the MH reservoir in the Nankai Trough, were selected as the host sands to produce MH bearing sands specimens. Suzuki et al. (Suzuki, et

al., 2009) investigated the grain size distribution range of core samples obtained from the Nankai Trough and initially named the five artificially prepared samples with representative grain size distribution curves from T_a to T_e . In this study, T_b and T_c were used as reconstituted samples. The artificially prepared sand T_b contains a smaller amount of fines content and has a

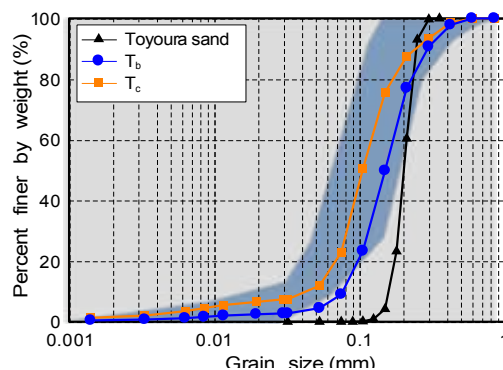


Figure 1 Grain size distribution curves

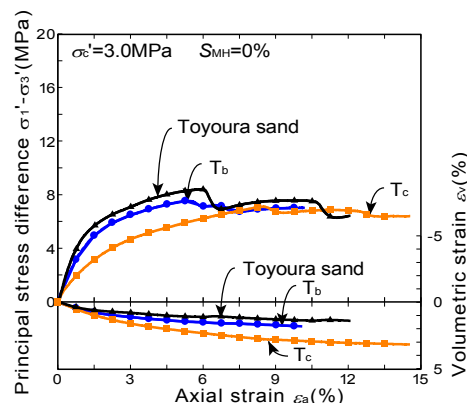


Figure 2 Stress-strain relationship of host sand

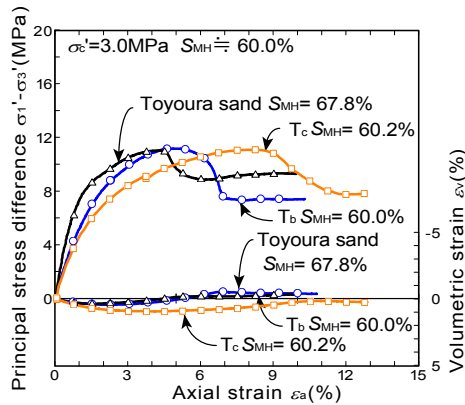


Figure 3 Stress – strain relationship of MH bearing sand

lower grain size distribution curve than T_c . Figure 1 shows the grain size distribution curves for all the host granular materials. The hatching area in Figure 1 represents the wide grain size distribution range of the MH concentrated sediment layers in the Nankai Trough. The testing apparatus used in this study can produce designated temperature and stress conditions of the MH reservoirs in the deep sea bed in order to create MH in the sand specimens. The testing apparatus was operated in a temperature-controlled room where the temperature can be controlled from 0 to 30°C. The specimen is 160 mm in height, 60 mm in width and 80 mm in depth. A 2.5 mm×2.5 mm grid is drawn on the front of the membrane. Confining plates are installed in both the front and back sides of specimens. The installation of the observation window in front of the specimen makes it possible to take pictures using a digital camera. The pressure applied on the specimen is controlled by the syringe pump. The pressure gauges are fixed on the top of the pressure cell and at the bottom of pressure cell. Variation in temperature of the specimen during generation and dissociation of MH is measured using thermocouples installed on the bottom pedestal. The observed images are analyzed using Particle Image Velocimetry (hereafter referred to as PIV) analysis to capture the local deformation of the specimen.

Initial water content was specially adjusted for each granular material specimen in order to achieve the target degree of MH saturation. The specimens were prepared using the wet tamping method, divided into 12 layers to reach a relative density of 90%. In order to produce MH, methane gas was continually injected into the specimen at a temperature of 5 °C for around 72 hours. Once MH had been formed, the gas in the pore spaces was replaced by the filtrated pore water, resulting in water saturation conditions. After this, the pore pressure was increased from 5 MPa to 10 MPa using the syringe pumps and a given effective confining stress was applied. Then, isotropic consolidation and drained shear and MH dissociation tests were performed. The constant shear strain rate applied on the specimen was 0.1 %/min. MH dissociation test were performed with shear stress. This shear stress was lower than the strength of MH bearing sand but higher than the strength of the corresponding host sand. Test was carried out using the same method

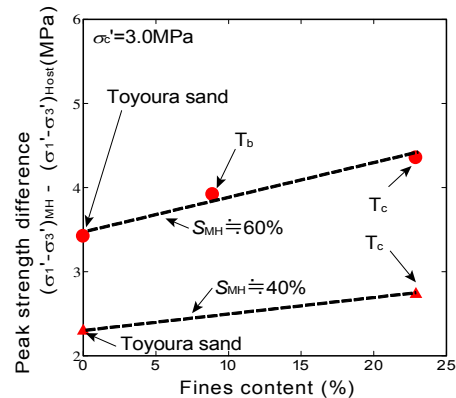
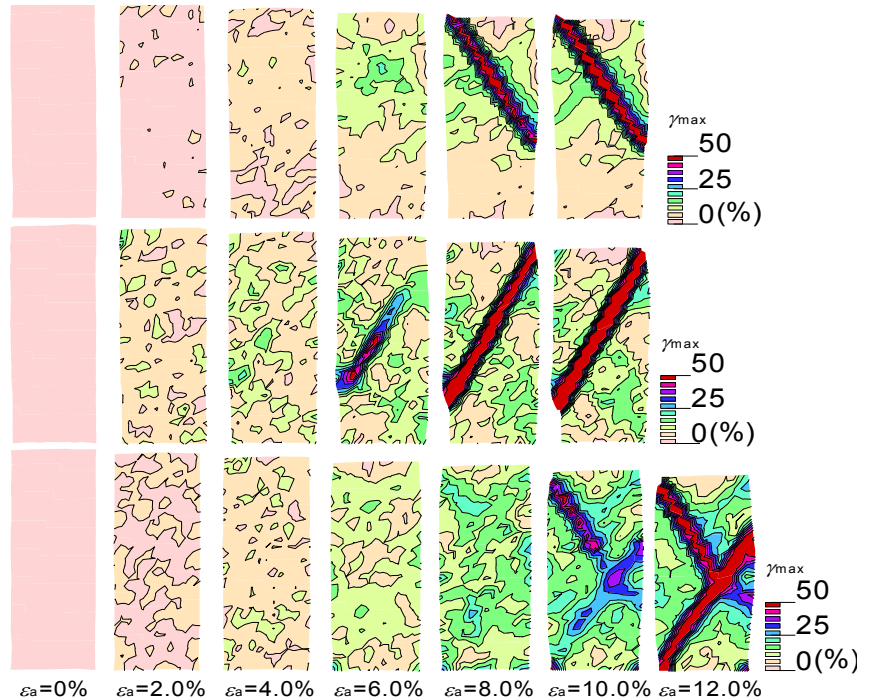


Figure 4 Strength increment by MH and fines content relationship


 Figure 5 The contour of maximum shear strain of Toyoura sand (upper), T_b (middle) and T_c (bottom)

adopted in the shearing test. The pore water pressure was reduced only in the upper side of the specimen from 10 MPa to 3 MPa at the constant shear stress which was previously provided. The pore water pressure was repressurized to 10 MPa after the completion of MH dissociation with the assumption of the abandonment of gas production well. The constant dissociation rate applied on the specimen was 0.5 MPa/min.

3 RESULT OF SHEAR TEST

The testing results of Toyoura sand, T_b and T_c host sands and MH bearing sands at an effective confining pressure of 3 MPa are presented in Figs. 2 and 3 respectively. In the case of MH bearing sands, the actual degree of MH saturation of Toyoura sand, T_b , T_c are 67.8 %, 60.0 % and 60.2 %. From Figure 2, initial stiffness and peak strength tended to increase with decreasing fines content. Furthermore, the axial strain corresponding to the peak strength of each specimen increases as the effective confining stress is increased in spite of the nearly same axial strain corresponding to the peak strength of Toyoura sand and T_b . The volumetric strain of all sands is purely contractive. This results from the occurrence of particle crushing at high

shear stresses. The contractive behaviour is predominant with increasing fines content. From Figure 3, the initial stiffness of sample with low fines content is higher and the peak strength of MH bearing sands is similar regardless of fines content. On the other hand, trend of the axial strain corresponding to the peak strength is similar to that of host sand. In comparison with host sand, the reducing tendency of contractive behaviour is observed. Figure 4 shows the relationship between the strength enhancement of MH bearing sands and axial strain. The strength enhancement is defined as the difference in peak strength of the MH bearing sand and that of the corresponding host sand. The shearing test results of MH bearing sands with the degree of MH saturation $S_{MH} \approx 40\%$ are also shown in Figure 4. The result demonstrates that the increasing fines content increases the axial level at which the largest strength enhancement appears regardless of the degree of MH saturation. This is assumed that fines become a cluster of grain particles cemented by MH and this structure contributes to the strength increment. Figure 5 shows the maximum shear strain contour from analytical results of Toyoura sand, T_b and T_c of MH bearing sand at axial strains from 0% to 10% at an increment of 2%. Here, although the maximum shear strain in the shear band exceeded 50%, the maximum value is limited to 50% in order to clearly show the even distribution of smaller shear strains. The variation of the maximum shear strain of each element of the specimen is evaluated from this contours. In this study, in order to evaluate the variation, it is assumed by Weibull modulus m . The Weibull distribution P_s can be expressed by the following form (Cheng et al., 2003).

$$P_s = \exp \left[- \left(\frac{\gamma}{\gamma_c} \right)^m \right] \quad (1)$$

Here, γ is the maximum shear strain of each element, γ_c is the average value of maximum shear strain. To determine Weibull modulus m in Formula (1), it is transformed to Formula (2).

$$\ln \left[\ln \left(\frac{1}{P_s} \right) \right] = m \ln \left(\frac{\gamma}{\gamma_c} \right) \quad (2)$$

From Formula (2), the least-squares regression had been done for the Weibull modulus m . Figure 6 shows the Weibull modulus of Toyoura sand at axial strain $\varepsilon_a = 2\%$ as an example. Figure 7 shows the Weibull distribution drawn with the Weibull modulus m obtained from Figure 6. From this figure, it is understood that variations from the average value is increased with the Weibull modulus m is decreasing. Figure 8 shows changing of Weibull modulus m with each axial strain. From Figure 8, it can be seen that variation of all sands is increased

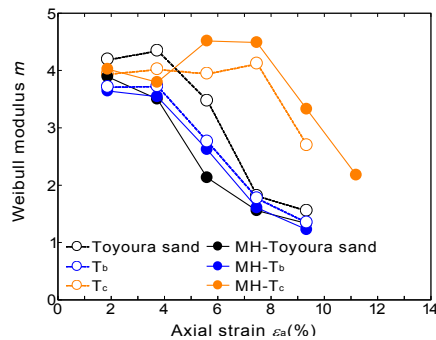


Figure 8 The changing of Weibull modulus

with increasing axial strain. The similar variable tendency of the degree of Weibull modulus for Toyoura sand and T_b with increasing axial strain is noticed. On the other hand, the degree of Weibull modulus of T_c is higher than that of other sands and variation is lesser than that of others. Furthermore, the degree of maximum shear strain of all sands is high at the center of shear band in Figure 5. In the case of T_c , the high maximum shear strain shows in wide area. In the case of Toyoura sand and T_b , the maximum shear strain of other part of shear band shows low. As a result, the local deformation of the specimen with low fines content is liable to occur.

4 RESULT OF MH DISSOCIATION TEST

The degrees of MH saturation of Toyoura sand, T_b and T_c are $S_{MH} = 60.3\%$, $S_{MH} = 57.3\%$, $S_{MH} = 41.3\%$ in advance of the MH dissociation. The relationship between the stress ratio and axial strain of Toyoura sand, T_b and T_c from shearing to repressurization are shown in Figure 9 – 11. In the case of T_b , when switching from shearing process to depressurizing process, MH has been generated in pipeline between the pressure gauge and syringe pump. The time passes to melt the MH in the pipeline as axial strain progresses. Additionally, the stress ratio for each host sand in shearing test is also shown. In each figure, point (a)

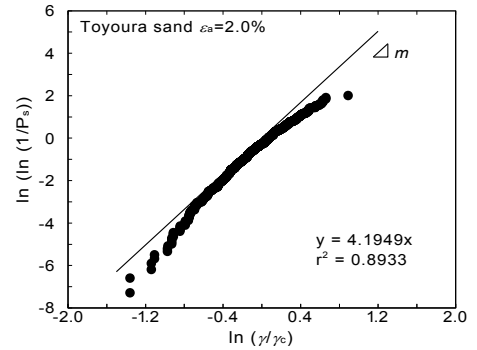


Figure 6 Weibull modulus of Toyoura sand at $\varepsilon_a = 2\%$

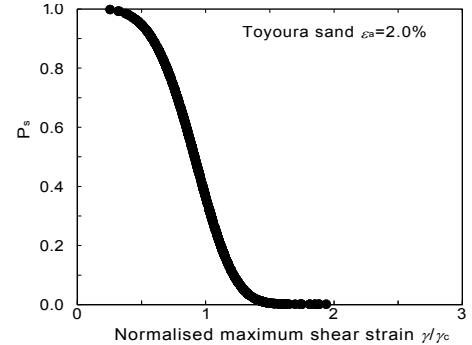


Figure 7 Weibull distribution of Toyoura sand at $\varepsilon_a = 2\%$

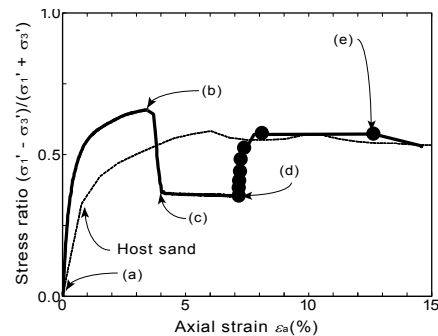
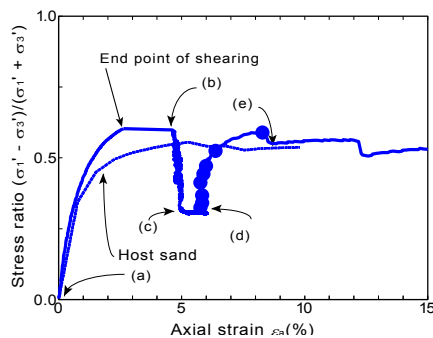
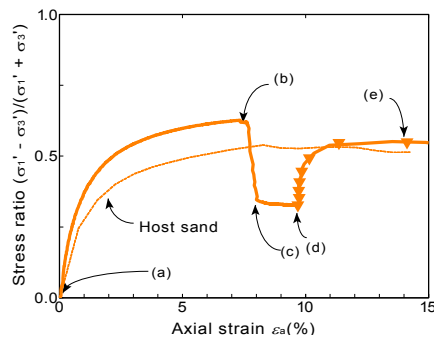
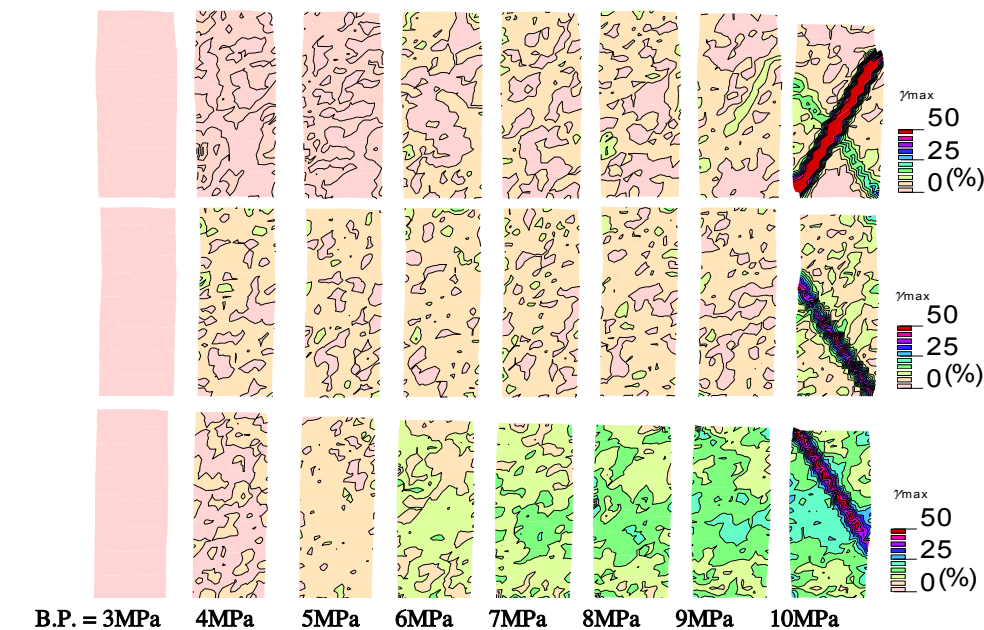


Figure 9 Relationship between stress ratio and axial strain (Toyouira sand)


 Figure 10 Relationship between stress ratio and axial strain (T_b)

 Figure 11 Relationship between stress ratio and axial strain (T_c)

corresponds to the point before dissociation, where initial shear stress has been applied. Point (b) corresponds to the point where pore water pressure is decreased from 10MPa to 3MPa. Point (c) corresponds to the point where MH is dissociated. Point (d) corresponds to the point where the specimen fails due to an increase in pore water pressure (repressurization). The plots of each figure show the pore water pressure in low stress ratio order from 3MPa to 10MPa. It can be seen that after depressurization, repressurization causes the specimens subjected to high initial shear stress to fail regardless of the existence of MH or not.


 Figure 12 The contour of maximum shear strain of Toyoura sand (upper), T_b (middle) and T_c (bottom) during repressurization

5 CONCLUSION

In this study, a series of shearing and dissociation tests were performed on MH bearing sand composed of three kinds of sands with various fines contents. The results gained from this study are concluded as follows:

- (1) The initial stiffness and peak strength of MH bearing sands increase and the volumetric strain varies from contractive to dilative behaviour with the increasing degree of MH saturation. The strength increment induced by MH increases with increasing fines content.
- (2) The variation in the maximum shear strain with low fines content increases with increasing axial strain. Furthermore, it is assumed that local deformation likely occurs near shear band for specimens with low fines content.
- (3) After depressurization, the repressurization causes the speci

men subjected to high shear stress to fail regardless of the existence of MH or not.

6 ACKNOWLEDGEMENTS

The present work was done as the activity of Research Consortium for Methane Hydrate Resources in Japan (MH21 Research Consortium) by the Ministry of Economy and Industry and the part of the work was supported by KAKENHI 25249065 and 15J06540 by the Ministry of Education and Science in Japan. The authors would like to express their sincere thanks to their supports.

7 REFERENCES

- MH21 Research Consortium 2014. <http://www.mh21japan.gr.jp/>
- Suzuki, K., Ebinuma, T. and Narita, H. 2009. Features of Methane Hydrate-bearing Sandy-sediments of the Forearc Basin along the Nankai Trough : Effect on Methane Hydrate-Accumulating Mechanism in Turbidite, *Journal of Geography*, 118 (5), 899-912. (in Japanese).
- Hyodo, M., Yoneda, J., Yoshimoto, N. and Nakata, Y. 2013. Mechanical and dissociation properties of methane hydrate-bearing sand in deep seabed, *Soils and Foundations*, 53(2), 299-314.
- Yoneda, J., Hyodo, M., Yoshimoto, N., Nakata, N., Kato, A. 2013. Development of high-pressure low-temperature plane strain testing apparatus for methane hydrate-bearing sand, *Soils and Foundations*, 53(5), 774-783.
- Cheng, Y., P., Nakata, Y., and Bolton, M., D. 2003. Discrete element simulation of crushable soil, *Geotechnique* 53(7), 633-641.